

Epidemic threshold influenced by non-pharmaceutical interventions in residential university environments

Zechao Lu(卢泽超), Shengmei Zhao(赵生妹), Huazhong Shu(束华中), and Long-Yan Gong(巩龙延)

Citation: Chin. Phys. B, 2024, 33 (**2**): 028707. DOI: 10.1088/1674-1056/ace2b0
Journal homepage: http://cpb.iphy.ac.cn; http://iopscience.iop.org/cpb

What follows is a list of articles you may be interested in

Impact of individual behavior adoption heterogeneity on epidemic transmission in multiplex networks

Liang'an Huo(霍良安) and Yue Yu(于跃)
Chin. Phys. B, 2023, 32 (**10**): 108703. DOI: 10.1088/1674-1056/acea65

Self-similarity of complex networks under centrality-based node removal strategy

Dan Chen(陈单), Defu Cai(蔡德福), and Housheng Su(苏厚胜)
Chin. Phys. B, 2023, 32 (**9**): 098903. DOI: 10.1088/1674-1056/acd3e2

Effective suppression of beta oscillation in Parkinsonian state via a noisy direct delayed feedback control scheme

Hai-Tao Yu(于海涛), Zi-Han Meng(孟紫寒), Chen Liu(刘晨), Jiang Wang(王江), and Jing Liu(刘静)
Chin. Phys. B, 2021, 30 (**3**): 038703. DOI: 10.1088/1674-1056/abd395

Computational study of non-catalytic T-loop pocket on CDK proteins for drug development

Huiwen Wang(王慧雯), Kaili Wang(王凯丽), Zeyu Guan(管泽雨), Yiren Jian(简弋人), Ya Jia(贾亚), Fatah Kashanchi, Chen Zeng(曾辰), Yunjie Zhao(赵蕴杰)
Chin. Phys. B, 2017, 26 (**12**): 128702. DOI: 10.1088/1674-1056/26/12/128702

Reverse-feeding effect of epidemic by propagators in two-layered networks

Dayu Wu(吴大宇), Yanping Zhao(赵艳萍), Muhua Zheng(郑木华), Jie Zhou(周杰), Zonghua Liu(刘宗华)
Chin. Phys. B, 2016, 25 (**2**): 028701. DOI: 10.1088/1674-1056/25/2/028701

Epidemic threshold influenced by non-pharmaceutical interventions in residential university environments

Zechao Lu(卢泽超)[1], Shengmei Zhao(赵生妹)[1], Huazhong Shu(束华中)[2], and Long-Yan Gong(巩龙延)[2,†]

[1] *Institute of Signal Processing and Transmission, Nanjing University of Posts and Telecommunications, Nanjing* 210003, *China*
[2] *College of Science, Nanjing University of Posts and Telecommunications, Nanjing* 210003, *China*

(Received 31 March 2023; revised manuscript received 5 June 2023; accepted manuscript online 29 June 2023)

The control of highly contagious disease spreading in campuses is a critical challenge. In residential universities, students attend classes according to a curriculum schedule, and mainly pack into classrooms, dining halls and dorms. They move from one place to another. To simulate such environments, we propose an agent-based susceptible–infected–recovered model with time-varying heterogeneous contact networks. In close environments, maintaining physical distancing is the most widely recommended and encouraged non-pharmaceutical intervention. It can be easily realized by using larger classrooms, adopting staggered dining hours, decreasing the number of students per dorm and so on. Their real-world influence remains uncertain. With numerical simulations, we obtain epidemic thresholds. The effect of such countermeasures on reducing the number of disease cases is also quantitatively evaluated.

Keywords: epidemic threshold, susceptible–infected–recovered model, non-pharmaceutical interventions, time-varying heterogeneous contact networks

PACS: 87.19.X–, 89.75.Hc, 87.23.Ge, 05.10.–a **DOI:** 10.1088/1674-1056/ace2b0

1. Introduction

In universities, the student population size is generally large, and students are in intimate contact, so infectious diseases spread more easily. Many research works have proposed models to study COVID-19 spread in such settings.[1–6] For instance, Hekmati *et al.* studied the airborne transmission risk associated with holding in-person classes on university campuses.[1] Borowiak *et al.* used mathematical models to evaluate strategies that suppress the spread of the virus, specifically in dorms and in classrooms.[2] When there is an epidemic outbreak, non-pharmaceutical interventions (NPIs) are effective methods to contain infection and delay spread, and include isolation of ill individuals, quarantine of exposed individuals, face mask usage, nucleic acid testing, cancellation of mass gatherings, and school and workplace closures.[7–12] However, their real-world influence remains uncertain.[13] It is interesting to propose models to give quantitative evaluations in university environments.

Epidemic threshold may be the important feature in the dynamics of an epidemic, which separates the healthy phase from the infected ones. To characterize it, mean-field compartmental models have been proposed and extensively studied,[14] where individuals belong to susceptible (S), infected (I), recovered (removed) (R), quarantine/isolation (Q), or other disease states (compartments). The population is supposed to be homogeneous mixing, and the evolutions of compartments are described by a group of non-linear differential coupling equations. For the SIR model,[15] the epidemic threshold $\lambda_c = 1$, where $\lambda = \beta/\mu$. In Ref. [16], β and μ are called transition rates for infection and recovery, and λ is called the spreading rate or effective infection rate.

In reality, individuals have large heterogeneity in social contact networks where diseases may propagate. The static or temporal network topology also influences epidemic thresholds.[16,17] For instance, under the mean field approximation, on static scale-free networks, it is found that $\lambda_c^{\rm SIS} = \lambda_c^{\rm SIR} = \langle k\rangle/\langle k^2\rangle$,[18,19] where k is the degree of nodes and $\langle\cdots\rangle$ denotes the mean value of corresponding quantities (the same below). By mapping the static uncorrelated networks onto a bond percolation problem, it is found that[20,21]

$$\lambda_c^{\rm SIR} = \frac{\langle k\rangle}{\langle k^2\rangle - 2\langle k\rangle}. \tag{1}$$

In fact, real contact networks are often time-varying ones, where links between nodes are temporally created, destroyed, or rewired.[16,17] For example, in an activity-driven contact network model,[22–24] at each time step, each node (individual) i becomes active with probability a_i. It generates m links that are connected to m randomly chosen nodes, and such links last for a period of time Δt. The more nodes are activated, the more links there are, so disease can easily propagate along such links. For such models, it is found that $\lambda_c^{\rm SIS} = \lambda_c^{\rm SIR} = \frac{1}{m\left(\langle a\rangle + \sqrt{\langle a^2\rangle}\right)}$.[24]

It is known that network structure and human mobility greatly influence the dynamics of an epidemic.[25,26] However, it is a challenge to create models that capture real-world dynamics in complex systems.[17] Traditional math models neglect the heterogeneity in social contact networks.[14,15] Static heterogeneous networks omit human mobility.[18–21] These

†Corresponding author. E-mail: lygong@njupt.edu.cn

© 2024 Chinese Physical Society and IOP Publishing Ltd

time-varying heterogeneous contact networks are far away from the real world.[22–24] In recent years, agent based, spatially structured models have attracted a lot of attention, where the discrete nature of individuals, their mobility and stochastic contacts are considered.[6,7,16] Such models can capture the spreading patterns at the level of single individuals. Based on such models, disease spreads in social networks are studied, such as households, schools, workplaces and stores.[7,16] Compared with other social networks, in universities the student population size is generally large, and students regularly have classes, have meals and go to sleep, where they are in intimate contact. So the university environment is a paradigm of temporal contact networks. With Monte–Carlo simulation methods, we will study how disease propagates in universities using the full-scale stochastic agent-based model.[6] In close environments, maintaining physical distancing is an available NPI and is the most often used. We consider NPIs including using larger classrooms, adopting staggered dining hours and/or decreasing the number of students per dorm. The influences on the epidemic thresholds are explored. The underlying mechanisms will provide scientific evidence to control epidemics in universities.

The remainder of the paper is organized as follows. In Section 2 we introduce the model and related quantities. In Section 3, we present the numerical results. Finally, we summarize and conclude in Section 4.

2. Model depiction and related quantities

We simulate the epidemic spread in residential universities with a full-scale stochastic agent-based model.[6] Monte–Carlo simulation methods are used. In models, we trace the movements of all students, which include having classes in classrooms, eating at dinner halls and sleeping in dorms; they randomly choose seats in classes and to have meals. We record everyone's health status, i.e., S, I or R, as they attend activities. Every day, the simulation data of the numbers of infected individuals and recovered individuals are collected. Details are as follows.

2.1. Disease spreading process

We presume the SIR disease spreading process.[14,16] At every moment, each individual belongs to the S, I or R disease state (compartment). For the n-th individual, this is represented by X_n, where $X = S, I$ or R and $n = 1, 2, \ldots, N$. Suppose that β and μ are the transition rates for infection and recovery.[16] For a time interval Δt, with transition probability $\beta\Delta t$, a susceptible individual will change to an infected one if he is in contact with infected individuals. The larger β is, the more easily the disease spreads among people. At the same time, infected individuals will recover their health with transition probability $\mu\Delta t$. And the recovered individuals will not be infected again. The variations of disease states can be written as

$$S_n(t) + \sum_m I_m(t) \xrightarrow{\beta\Delta t} I_n(t+\Delta t) + \sum_m I_m(t+\Delta t), \tag{2a}$$

$$I_n(t) \xrightarrow{\mu\Delta t} R_n(t+\Delta t), \tag{2b}$$

$$R_n(t) \xrightarrow{100\%} R_n(t+\Delta t), \tag{2c}$$

where the m-th individual with state I is the person in contact with the n-th individual. In simulations, after Δt, disease states for all people simultaneously update.

2.2. Time-varying and heterogeneous contact networks in residential universities

There are a large number of individuals, including students, faculty, and staff, in campuses. Due to a high student-faculty ratio at universities, for simplicity we only consider the behaviors of students.[1] Each student is enrolled in a class. Students go to classes according to their class schedules. Schedules are regular for every week. For some courses, students may have joint classes. The members are fixed for each course. We suppose all students have their breakfast, lunch, and supper at dining halls, and at dining tables they may touch students of other classes. Each student is assigned a dorm, and the roommates are fixed.

Students mainly pack into classrooms, dining halls or dorms. Due to epidemic prevention, they are loosely connected in other zones. As pointed out in Ref. [27], on the weekends, the contact networks in universities are more loosely connected, with fewer users interacting with study participants. At the same time, school administrators advise students to maintain social distancing. So, for simplicity, during these times, except for bedtime in dorms, we omit disease spreading, but individuals can recover. If an individual enters a zone, the individual randomly selects a position and stays there until he/she leaves the zone.[6] Students move from one zone to another ones. For an individual, the people he/she is in contact with and the number of people will vary with time. In this sense, his/her contact networks are time-varying and heterogeneous.

2.3. Procedure of simulation

Suppose a residential university has N_c classes. It has statistical data about the (frequency) distribution of weekly class hours ρ_{wch}, the distribution of class size ρ_{cs} and the distribution of the number of joint classes ρ_{njc}. It also provides the school's daily schedule.

Triple parameters (η_c, η_d, n_d) are introduced, which are the seat occupancy rate in classrooms, the seat occupancy rate in dining halls and the number of students per dorm, respectively. They can be taken as averaged values of corresponding

quantities. First, they relate to the degree of subnetworks. Second, they quantitatively characterize classroom capacity, staggered dining hours and dorm capacity, which relate to NPIs. So they are important parameters in our models.

Each classroom and each dining hall are simulated by square lattice networks. If an individual stays at lattice (i,j), the nearest and next nearest lattices $(i\pm1,j)$, $(i,j\pm1)$ or $(i\pm1,j\pm1)$ may be occupied. He/she is in contact with the individuals who stay at these lattices, and the individuals at other lattices are omitted. Each dorm is simulated by a fully connected network, i.e., an individual is in contact with all the other members of the dorm.

The procedure of stochastic simulation is as follows:

(i) The number of classes $N_{\rm c}$ is set. Class sizes are randomly selected from the distribution of class size $\rho_{\rm cs}$. Each student is assigned a unique identifier number n.

(ii) A class schedule is generated for each class. Weekly class hours are randomly selected from the distribution $\rho_{\rm wch}$. For each course, joint classes are randomly selected from the distribution $\rho_{\rm njc}$. Based on the school's daily schedule, the time for each course is randomly arranged. In a classroom, the number of seats $n^{\rm c}_{\rm seat}=[\rho_{\rm cs}\rho_{\rm njc}/\eta_{\rm c}]$, where $[z]$ denotes the integer of z. In dining halls, the number of seats $n^{\rm d}_{\rm seat}=N/\eta_{\rm d}$. In classrooms and dining halls, students randomly choose seats. And there are $n_{\rm d}$ students in each dorm.

(iii) The recovery rate μ and the effective transmission rate λ are set. Then the infected rate $\beta=\lambda\mu$.

(iv) Initially, one student is randomly selected from all N students and we set his/her disease state as I and all other students' states as S.

(v) From Monday to Sunday, based on the school's daily schedule and the class schedules, an individual goes to dining halls, goes to classrooms if he/she has classes, stays at dorms, and so on.

If an individual stays in one zone for a time interval Δt, a susceptible individual becomes infected at a rate $\beta\Delta t$ if he/she is in contact with infected individuals, an infected individual becomes a recovered one at a rate $\mu\Delta t$, and a recovered individual stays recovered [see Eq. (2)]. (Disease) states of all individuals are updated in parallel.

(vi) Repeat the (v)-th step until there are no infected individuals, then simulation for one cycle is completed.

(vii) Repeat steps (i)–(vi) to apply simulation for other cycles.

University environments are temporal contact networks, where the prevalence rate of COVID-19 depends on the infected rate, the recovery rate, the contact rate of individuals, and others. In the models, the infected rate β and the recovery rate μ are independent variables. Recovery time from a disease depends on ages, overall health and other factors. For COVID-19, research suggests that it could take 2 weeks for someone to get over a mild illness or up to 6 weeks for severe or critical cases.[28] In our studies, to reduce the number of parameters, we fix $\mu=1/14$ day^{-1} and vary β. At the same time, we define the effective infected rate $\lambda\equiv\beta/\mu$,[16] so it is a tunable parameter. The larger λ is, the larger the probability an individual may be infected.

In simulations, everyone's disease state evolves based on Eq. (2). The time interval $\Delta t=45$ mins for each class, $\Delta t=30$ min for each meal, and $\Delta t=8$ hours for sleep. In numerical simulations, we transfer all units to minutes. The system works day after day and week after week, until there are no infected individuals. At 22:30 every day, the data of the number of infected individuals and recovered individuals are collected, which will be used to characterize dynamic behaviors of systems.

2.4. Related quantities

For SIR models, $N_S(t)+N_I(t)+N_R(t)=N$, where $N_S(t),N_I(t)$ and $N_R(t)$ are the number of individuals with state S,I and R, respectively. As t increases, $N_S(t)$ will decrease, $N_R(t)$ will increase, and N_I first increases to a peak, then decreases to zero.[16] After enough time, there are no infected individuals. The final epidemic size is defined by

$$r_\infty=\frac{N_R(t\to\infty)}{N}. \tag{3}$$

In fact, r_∞ can play the role of an order parameter to detect healthy-infected phase transitions.[16] In healthy phases, r_∞ are zeros, or are very small and can be ignored. In infected phases, r_∞ are finite values.

The fluctuations of final epidemic sizes are often large near the epidemic threshold. In order to identify the epidemic thresholds in finite system sizes, we also study the variability of r_∞, which is defined by[29–32]

$$\Delta=\frac{\sqrt{\langle r_\infty^2\rangle-\langle r_\infty\rangle^2}}{\langle r_\infty\rangle}. \tag{4}$$

Here $\langle z\rangle$ is the ensemble average of z. In physics, it is a standard method to determine the critical point in the equilibrium phase of a magnetic system.[33] It may exhibit a peak at $\lambda_{\rm p}$. For finite systems, it is used to approximate the epidemic threshold $\lambda_{\rm c}$. The validity of the numerical identification method has been confirmed for the SIR model in network models.[31]

The outbreak duration τ is another basic quantity.[16] When a system approaches a critical transition or a tipping point, the system may return more slowly to its stable states under small perturbations,[34] i.e., the critical slowing down phenomenon. It can be used as early warning signals of infectious disease transitions.[35] We use the definition in Ref. [32], which is

$$\tau^2=\int_0^\infty t^2\phi(t)\,{\rm d}t-\left[\int_0^\infty t\phi(t)\,{\rm d}t\right]^2, \tag{5}$$

where

$$\phi(t) = \frac{P(t)}{\int_0^\infty P(t')\,\mathrm{d}t'}, \quad P(t) = N_I(t)/N.$$

3. Results

The reality of Nanjing University of Posts and Telecommunications (NJUPT) is used as an example. In Figs. 1(a)–1(c), we plot the distribution of weekly class hours $\rho_{\rm wch}$, the distribution of class size $\rho_{\rm cs}$, and the distribution of the number of joint classes $\rho_{\rm njc}$, respectively. From Fig. 1(b), we find that the mean number of students in each class is 31.9.

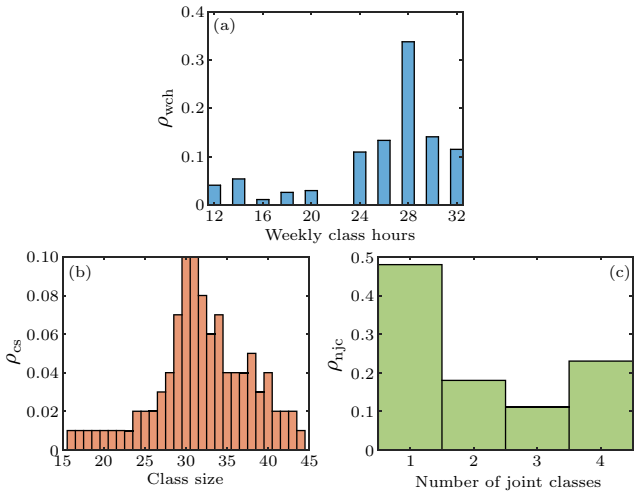


Fig. 1. (a) The distribution of weekly class hours $\rho_{\rm wch}$, (b) the distribution of class size $\rho_{\rm cs}$, and (c) the distribution of the number of joint classes $\rho_{\rm njc}$, respectively.

From Monday to Friday, the school's daily schedule is as follows: 7:00–7:30 breakfast; 8:00–8:45, 8:50–9:35, 9:50–10:35, 10:40–11:25 and 11:30–12:15 are the 1st to 5th classes, respectively; 12:30–13:00 lunch break; 13:45–14:30, 14:35–15:20, 15:35–16:20 and 16:25–17:10 are the 6th to 9th classes, respectively; 17:30–18:00 supper break; 18:30–19:15, 19:25–20:10 and 20:20–21:05 are the 10th to 12th classes; 22:30–6:30 sleeping.

3.1. No interventions

Based on the resources (the number of classrooms, dining rooms and dorms) of NJUPT and the total number of students in NJUPT, we set $(\eta_{\rm c}, \eta_{\rm d}, n_{\rm d}) = (0.8, 0.7, 6)$, which is the baseline scenario, i.e., the no interventions case. Results are shown in Fig. 2. For each λ, data for 100 cycles of stochastic simulations are given. More simulation cycles give similar results. The vertical blue lines are for the function $\lambda = 0.52$.

In detail, the final epidemic size r_∞ versus the effective infected rate λ is plotted in Fig. 2(a). It shows that data almost overlap for the number of classes $N_{\rm c} = 150$, 300 and 600, which means such sizes can reflect statistical properties of systems. When λ is relatively small, r_∞ is relatively small and approaches zero, which corresponds to the healthy phase. When λ is relatively large, the values of r_∞ are divided into two branches: in the bottom one, r_∞ is relatively small and approaches zero,[36] and in the top one, r_∞ is finite and increases with λ, which corresponds to the infected phase. In fact, r_∞ plays the role of order parameter to detect phase transitions.[16] The epidemic threshold $\lambda_{\rm c}$ determined by r_∞ should be in the thermodynamic limit.[16] For finite systems, Fig. 2(b) shows that the variability Δ exhibits a peak at $\lambda = 0.52$, which is used to approximate $\lambda_{\rm c}$.[29–32] As there are two branches in r_∞ at relatively large λ, in calculating Δ, data for $r_\infty > 0.05$, i.e., the top branch of r_∞, are considered. Further, Fig. 2(c) shows that the outbreak duration τ is maximal near $\lambda = 0.52$, which also signals the epidemic threshold.

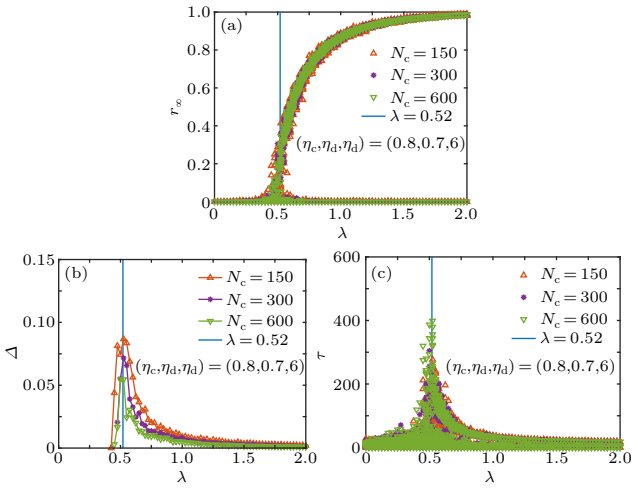


Fig. 2. (a) The final epidemic size r_∞, (b) the variability Δ and (c) the outbreak duration τ versus the effective infected rate λ at $(\eta_{\rm c}, \eta_{\rm d}, n_{\rm d}) = (0.8, 0.7, 6)$, respectively. The number of classes $N_{\rm c} = 150$, 300 and 600, respectively. The vertical blue lines are for the function $\lambda = 0.52$. Data for 100 stochastic simulations are given.

3.2. Non-pharmaceutical interventions

We set $(\eta_{\rm c}, \eta_{\rm d}, n_{\rm d})$ equal to $(0.8, 0.3, 6)$, $(0.8, 0.7, 3)$, $(0.4, 0.7, 6)$ and $(0.4, 0.3, 3)$, respectively, which are labeled NPI-I, NPI-II, NPI-III and NPI-IV scenarios, respectively. At least one of their components is smaller than that for the baseline scenario [no interventions, $(\eta_{\rm c}, \eta_{\rm d}, n_{\rm d}) = (0.8, 0.7, 6)$]. In practice, the methods of small class teaching (or being designated a larger classroom), staggered dining hours, and renting social housing can realize the required conditions.

For the four NPI scenarios, we plot the final epidemic size r_∞ versus the effective infected rate λ in Fig. 3. The number of classes $N_{\rm c} = 300$ is used as an example. For each scenario, there exists an epidemic threshold $\lambda_{\rm c}$ separating the healthy phase from the infected phase, which is labeled by a vertical blue line. The corresponding $\lambda_{\rm c}$ can be numerically estimated from Figs. 4 and 5, at which the variability Δ and the outbreak duration τ exhibit peak values. In calculating Δ, data for $r_\infty > 0.05$ are taken into consideration.

Eqnarray (1) gives the theoretical prediction of $\lambda_{\rm c}$ for static uncorrelated networks.[20,21] As the underlying net-

works we study are time-varying heterogeneous contact ones,

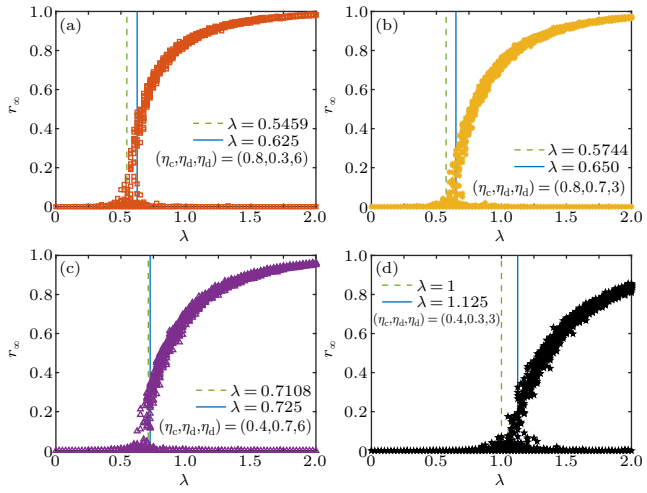


Fig. 3. The final epidemic size r_∞ as a function of the effective infected rate λ for (η_c,η_d,n_d) equal (a) $(0.8,0.3,6)$, (b) $(0.8,0.7,3)$, (c) $(0.4,0.7,6)$ and (d) $(0.4,0.3,3)$, respectively. The number of classes $N_c = 300$. The vertical lines are for some values of λ. Data for 100 stochastic simulations are given.

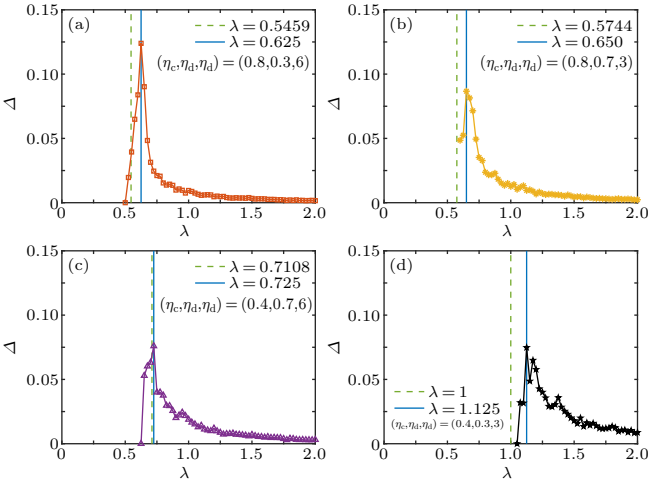


Fig. 4. The same as Fig. 3, but the variability Δ as a function of the effective infected rate λ.

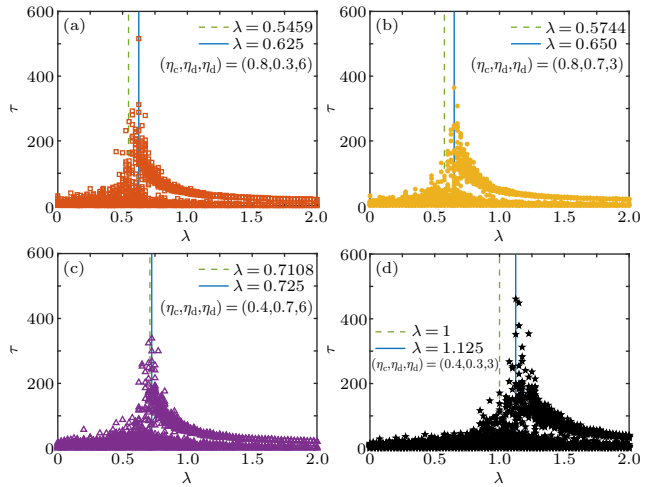


Fig. 5. The same as Fig. 3, but the outbreak duration τ as a function of the effective infected rate λ.

inspired by Eq. (1) we define

$$\lambda_t = \frac{\langle k\rangle_t}{\langle k^2\rangle_t - 2\langle k\rangle_t}, \tag{6}$$

where k is the degree of nodes and $\langle\cdots\rangle_t$ denotes the time mean of the corresponding quantities. At the healthy-infected phase transition point,

$$\lambda_t = \frac{\langle\beta\rangle_t}{\langle\mu\rangle_t} = \frac{\beta W}{\mu} = \lambda_c^t W. \tag{7}$$

In our model, students have much leisure time and during these times individuals can recover but not be infected. So W is the ratio of the time spent having classes, having dinner and sleeping in dorms to all time. On the other hand, at $\beta/\mu > 1$, i.e., infected rate β is greater than recovery rate μ, due to the heterogeneity and randomness in social contact networks, a finite value of r_∞ may occasionally occur. Combining the two aspects, the epidemic threshold can be approximately evaluated by

$$\lambda_c^* = \min\{\lambda_c^t, 1\} = \min\{\lambda_t/W, 1\}. \tag{8}$$

In Figs. 3–5, λ_c^* are labeled by vertical green dashed lines. Simulation results certify the argument and Eq. (8). They show λ_c^* are the lower bounds of epidemic thresholds.

3.3. Comparing no interventions with non-pharmaceutical interventions

Table 1 gives the epidemic thresholds λ_c^* obtained from Eq. (8) and the epidemic thresholds λ_c numerically estimated by the peaks of the variability Δ (the outbreak duration τ). At the same time, to illustrate visually differences between them, we also plot the bar graph for λ_c^* and λ_c in Fig. 6. From them, we find NPIs can raise epidemic thresholds. In the NPI-III scenario, larger classrooms are used. Compared with the NPI-I and NPI-II scenarios, λ_c^* (λ_c) is relatively large in the NPI-III scenario, so its effect on containing infection is relatively obvious. The reason is that classrooms are the main places that students stay and contagious disease spreads. Combination of interventions is the NPI-IV scenario and the corresponding effect is most significant.

Table 1. Table outlining the values of λ_c^* and λ_c.

Scenario	(η_c,η_d,n_d)	λ_c^*	λ_c
Baseline	$(0.8,0.7,6)$	0.5229 ± 0.0009	0.520
NPI-I	$(0.8,0.3,6)$	0.5459 ± 0.0009	0.625
NPI-II	$(0.8,0.7,3)$	0.5744 ± 0.0015	0.650
NPI-III	$(0.4,0.7,6)$	0.7108 ± 0.0011	0.725
NPI-IV	$(0.4,0.3,3)$	1	1.125

For all scenarios, including no interventions and NPIs, the final epidemic sizes r_∞ are plotted together in Fig. 7(a). The mean $\langle r_\infty\rangle$ are also shown in Fig. 7(b), where data for $r_\infty > 0.05$ are taken into consideration. To give quantitative comparisons, we define the ratio

$$K = \frac{\langle r_\infty\rangle_{(\eta_c,\eta_d,n_d)}}{\langle r_\infty\rangle_{(\eta_c=0.8,\eta_d=0.6,n_d=6)}}. \tag{9}$$

We plot the corresponding ratio K in Fig. 7(c). This shows that at relatively small λ, the effect of countermeasures is more obvious. All NPIs can reduce the outbreak size. For the combination of interventions, i.e., $(\eta_c, \eta_d, n_d) = (0.4, 0.3, 3)$, $K = 7.8\%$ at $\lambda = 1$ and $K = 84.9\%$ at $\lambda = 2$, which has the most significant effect in reducing the outbreak size.

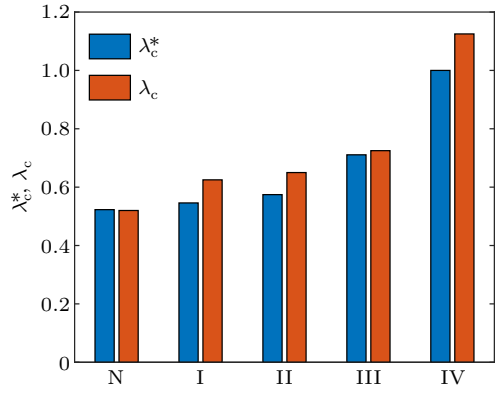


Fig. 6. The bar graph for λ_c^* and λ_c, where N denotes the baseline scenario, and I–IV denote the NPI-I–IV scenarios.

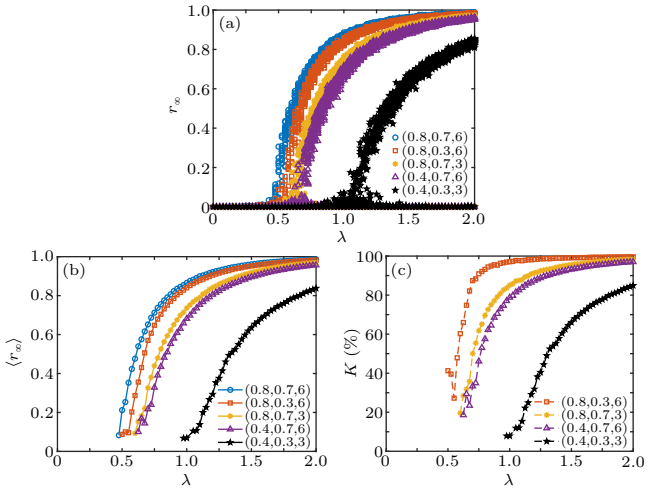


Fig. 7. (a) The final epidemic size r_∞, (b) the mean $\langle r_\infty \rangle$, and (c) the ratio K versus the effective infected rate λ, respectively, where (η_c, η_d, n_d) equals $(0.8, 0.7, 6)$, $(0.8, 0.3, 6)$, $(0.8, 0.7, 3)$, $(0.4, 0.7, 6)$ and $(0.4, 0.3, 3)$. The number of classes $N_c = 300$. Data for 100 stochastic simulations are given.

4. Conclusion

The university is a typical social community. To quantitatively evaluate the effect of NPIs on containing infection, an agent-based SIR model with time-varying heterogeneous contact networks is proposed. The seat occupancy rate in classrooms, the seat occupancy rate in dining halls and the number of students per dorm are important parameters to characterize NPIs. We obtain epidemic thresholds for scenarios including no interventions and four kinds of NPIs. We make quantitative comparisons. We find the NPI of using larger classrooms plays an important role in raising the epidemic threshold and reducing the outbreak size. In fact, it can also be realized by reducing the number of students in a classroom, i.e., dividing a class into several small classes. The effect of combination of interventions is most significant. All these studies provide scientific evidence to support the use of NPIs in campuses.

Acknowledgment

Project supported by the National Natural Science Foundation of China (Grant No. 61871234).

References

[1] Hekmati A, Luhar M, Krishnamachari B and Matarić M 2021 *IEEE International Conference on Communications Workshops* (ICC Workshops) pp. 1–6
[2] Borowiak M, Ning F, Pei J, Zhao S, Tung H and Durrett R 2021 *Math. Biosci. Eng.* **18** 551
[3] Brooks-Pollock E, Christensen H, Trickey A, Hemani G, Nixon E, Thomas A C, Turner K, Finn A, Hickman M, Relton C and Danon L 2021 *Nat. Commun.* **12** 5017
[4] Frazier P I, Cashore J M, Duan N, Henderson S G, Janmohamed A, Liu B, Shmoys D B, Wan J and Zhang Y 2022 *Proc. Natl. Acad. Sci. USA* **119** e2112532119
[5] Gressman P T and Peck J R 2020 *Math. Biosci.* **328** 108436
[6] Ranoa D R E, Holland R L, Alnaji F G, *et al.* 2022 *Nat. Commun.* **13** 3207
[7] Perra N 2021 *Phys. Rep.* **913** 1
[8] Lai S, Ruktanonchai N W, Zhou L, *et al.* 2020 *Nature* **585** 410
[9] Xiao T, Mu T, Shen S, Song Y, Yang S and He J 2022 *Physica A* **592** 126734
[10] Gaetaa G 2020 *Chaos, Solitons and Fractals* **140** 110074
[11] d'Onofrio A and Manfredi P 2022 *Chaos, Solitons and Fractals* **159** 112072
[12] Tong Y H, King C and Hu Y H 2021 *Chin. Phys. B* **30** 098903
[13] Ge Y, Zhang W, Wu X, *et al.* 2022 *Nat. Commun.* **13** 3106
[14] Martcheva M 2015 *An Introduction to Mathematical Epidemiology* (New York: Springer)
[15] Kermack W O and McKendrick A G 1927 *Proc. R. Soc. London A: Math. Phys. Eng. Sci.* **115** 700
[16] Pastor-Satorras R, Castellano C, Van Mieghem P and Vespignani A 2015 *Rev. Mod. Phys.* **87** 925
[17] Leitch J, Alexander K A and Sengupta S 2019 *Appl. Netw. Sci.* **4** 105
[18] Pastor-Satorras R and Vespignani A 2001 *Phys. Rev. Lett.* **86** 3200
[19] Moreno Y, Pastor-Satorras R and Vespignani A 2002 *Eur. Phys. J. B* **26** 521
[20] Newman M E J 2002 *Phys. Rev. E* **66** 016128
[21] Hasegawa T and Nemoto K 2016 *Phys. Rev. E* **93** 032324
[22] Perra N, Gonçalves B, Pastor-Satorras R and Vespignani A 2012 *Sci. Rep.* **2** 469
[23] Liu S, Perra N, Karsai M and Vespignani A 2014 *Phys. Rev. Lett.* **112** 118702
[24] Starnini M and Pastor-Satorras R 2014 *Phys. Rev. E* **89** 032807
[25] Cui Y P, Ni S J and Shen S F 2021 *Chin. Phys. B* **30** 048901
[26] Peng X L and Zhang Y D 2021 *Chin. Phys. B* **30** 058901
[27] Hambridge H L, Kahn R and Onnela J P 2021 *Int. J. Infect. Dis.* **113** 325
[28] https://www.webmd.com/covid/covid-recovery-overview
[29] Crépey P, Alvarez F P and Barthélemy M 2006 *Phys. Rev. E* **73** 046131
[30] Shu P, Tang M, Gong K and Liu Y 2012 *Chaos* **22** 043124
[31] Shu P, Wang W, Tang M and Do Y 2015 *Chaos* **25** 063104
[32] Silva D H, Anteneodo C and Ferreira S C 2023 *Commun. Nonlinear. Sci. Numer. Simula.* **116** 106877
[33] Landau D and Binder K 2009 *A guide to Monte Carlo simulations in statistical physics*, 3rd edn. (Cambridge University Press, New York)
[34] Nazarimehr F, Jafari S, Perc M and Sprott J C 2020 *Europhys. Lett.* **132** 18001
[35] Southall E, Brett T S, Tildesley M J, Dyson L. 2021 *J. R. Soc. Interface* **18** 20210555
[36] Due to the stochastic effect brought by the underlying networks and initial conditions (only one infected seed, see the 4-th step of the simulation procedure given in Subsection 2.3), r_∞ may be small even at large λ.